

Synthesization of Cerium Doped Nano Zinc Cobalt Ferrite for Voc Sensor Studies

¹C.Balakumar

¹Assistant Professor in ECE Department, St. Michael College of Engineering & Technology
St. Michael College of Engineering & Technology, Santhiagappar Nagar, Kalayarkoil, Tamil Nadu 630551

Submitted: 10-08-2021

Revised: 22-08-2021

Accepted: 25-08-2021

ABSTRACT: The magnetic properties of Zn-ferrite ceramics $Zn_{1-x-y}Co_yCe_xFe_2O_4$, (where $x = 0.012, 0.014, 0.016, 0.018$ and $y = 0.001, 0.001, 0.014, 0.016$) were synthesized by sol gel auto combustion method. The structure and composition of Ce doped Zn-ferrite ceramics was analyzed and the nano size was confirmed by the SEM monographs. The VSM studies confirm the magnetic behaviour and used to understand the electromagnetic properties of these nano materials.

Key words: Ferrimagnetic materials; Nanomaterials; Magnetization, VSM, SEM

I. INTRODUCTION

In advanced technologies the ferrites are used for magnetic or electrical applications, as they are the required high-density materials [1-3]. Synthesis of nanometer size particles proved to be one of the interesting fields of material science in material processing and technological applications, as the small size particles have some of the interesting properties as compared to bulk particles. These particles have improved catalytic, dielectric and magnetic, properties, as they possess high resistivity and negligible eddy current losses [4]. Magnetic nano particles promise some interesting applications, such as in high frequency devices, magnetic fluids, high density magnetic recording, colour imaging etc[5-9]

The various processing techniques, which are used for the synthesis of spinel ferrite powders include microwave refluxing[10] , sol-gel[11], hydrothermal[12], co-precipitation [13], spray pyrolysis[14]. In fact there are numerous papers on synthesis of Zinc ferrite by various methods. In the present investigation we have employed sol-gel auto-ignition method to synthesize Ce doped Zinc ferrite nanoparticles. The sol-gel auto-ignition method is used to speed up the synthesis of complex materials. It is a simple process, which offers a significant saving in time and energy consumption over the traditional methods, and

requires less sintering temperature. This method is employed to obtain improved powder characteristics, more homogeneity and narrow particle size distribution, thereby influencing structural, electrical, and magnetic properties of spinel ferrites. We examined the microstructures of the end products by X-ray diffraction and SEM to obtain quasi-three dimensional information on the grain shape, size and pore sizes[15]. It has been already reported that Zinc ferrite is an n type semi conductor with a band gap of 3.37eV[16-17]. Cerium-substituted ferrite, in particular, has been found to exhibit a large magneto-optic effect and low propagation loss, which will be good candidate materials for the devices with higher quality [18,19]. A low coercivity, high-remenance, soft magnetic material, having a hysteresis loop, is required for microwave operation. For a magnetic material to be applied in microwave devices, the most important static magnetic properties are the saturation magnetization (Ms), anisotropy constants, Neel temperature, remanent magnetization, coercivity (Hc). In general, Ms and Hc are required for applications [20].

II. EXPERIMENTAL PROCEDURE

2.1 Synthesis Technique

Nanocrystalline powders of $Zn_{1-x-y}Co_yCe_xFe_2O_4$, (where $x = 0.012, 0.014, 0.016, 0.018$ and $y = 0.001, 0.001, 0.014, 0.016$) were prepared by sol-gel auto-ignition method. The metal nitrates were dissolved together in a minimum amount of de-ionized water to get a clear solution. An aqueous solution of citric acid was mixed with metal nitrates solution, then ammonia solution was slowly added to adjust the pH to 7. The mixed solution was moved on to a hot plate with continuous stirring at 94°C. The viscous brown gel burnt with glowing flints. The auto ignition was completed within a minute, yielding into brown-colored ash. The as-prepared powders of all the samples were sintered in a microwave furnace

VBCC/MF to a temperature of 600°C for 1.5 hours. The grain size of the nanoferrite is determined using Scherrer's equation. The FWHM value of the peak corresponding to plane was considered after correction for instrumental broadening. Using the knowledge of site preference of the ions and the ionic size data of the respective ions, the cation distribution has been estimated theoretically using the following formula proposed [21, 22]. Mentioned in Table.2

$$\eta = \frac{M_w \times M_s}{5585}$$

Where M_w is the molecular weight of the sample and M_s is the saturation magnetization in emu/g.

2.2 FTIR study

Infrared absorption spectra in the range of $3.72 \times 10^4 \text{ m}^{-1}$ to $5.43 \times 10^4 \text{ m}^{-1}$ were recorded at room temperature by using SHIMADZU FTIR spectrum one spectrometer using KBr pellet method. The spectrum transmittance (%) against wave number (m^{-1}) is used for interpretation of the results.

2.3 SEM Studies

Micrographs of the sensor were recorded using a scanning electron microscope (HITACHI model S-3000H).

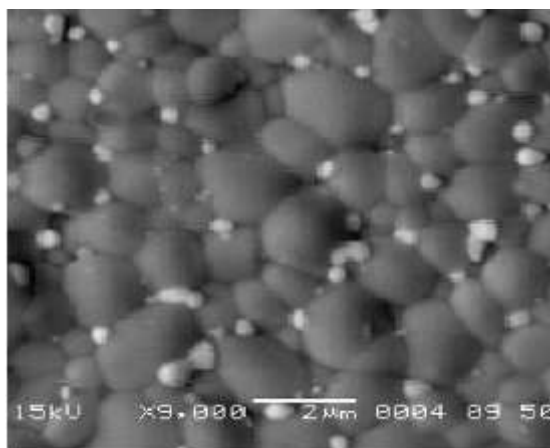


Fig.1 $\text{Zn}_{1-x-y}\text{Co}_y\text{Ce}_x\text{Fe}_2\text{O}_4$ $x=0.016, y=0.014$

The grains in the unsubstituted sample are inhomogeneous i.e., the grains are affected by certain stress, while the grains for the Fe substituted sample are nearly homogeneous due to the decrease of stress. The photographs confirm these results that the stability increased for substituted samples.

3.2 Hysterisis studies

2.4 Magnetic Measurements

The Magnetic measurements were performed using the commercial vibrating sample magnetometer (VSM) Lakeshore (Model73009). Magnetic hysteresis loops were measured at room temperature with maximal applied magnetic fields up to 0.95T. Magnetic field sweep rate was 5 Oe/s for all measurements, so that the measurement of hysteresis loops with maximum field of 0.989 T took about three hours.

III. RESULTS AND DISCUSSION

3.1 SEM analysis

Fig. 1 shows the microstructure of sintered specimen. Unsubstituted specimen (Fig.1) shows the presence of a monophasic homogeneous microstructure with an average grain size 0.42nm. Whereas, Ce-doped specimens' show a bi-phasic microstructure constituted of dark ferrite matrix grains and small whitish grain at the grain junction/boundary. As proposed by Sattar et, al [23] .This is due to the fact that the tetrahedral sites are small to be occupied by the large rare earth ions which have large ionic radius. Of course the probability of occupancy of the octahedral (B-site) by the rare earth ions will increase with decrease in the R ionic radius. This indicated whitish grains were CeFeO_3 .

Fig. 3,4 shows the variation in saturation magnetization (M_s) for the different x values of $\text{Zn}_{1-x-y}\text{Co}_y\text{Ce}_x\text{Fe}_2\text{O}_4$ ferrite, the saturation magnetization (M_s) value increases with increase in the value of x in Table.1.

The increasing Cerium content induced a polar-to-nonpolar phase transition. Within the polar region, a rhombohedral and two orthorhombic modifications of $\text{Zn}_{1-x-y}\text{Co}_y\text{Ce}_x\text{Fe}_2\text{O}_4$ were

found. It was shown that Cerium substitution resulted in the appearance of spontaneous magnetization, which was significantly enhanced

upon the composition-driven transition from a rhombohedral to an orthorhombic phase.

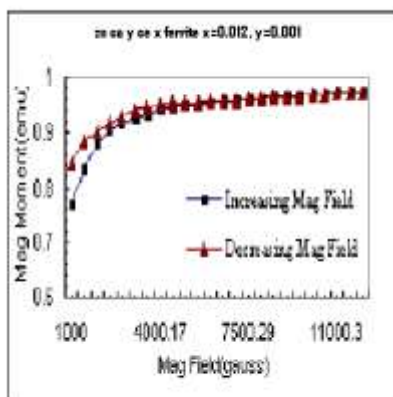


Fig.2 $Zn_{1-x-y}Co_yCe_xFe_2O_4$ $x=0.012, y=0.001$ Saturation magnetization (Ms)

Table 1 show that the change in retentivity and change of coercive force with change in concentration respectively. The coercive force show linear increase initially and later shows a gradual decrease with the increase in the dopant concentration. The values of magnetic parameters such as M_s , H_C , M_R of nano particles of $Zn_{1-x-y}Co_yCe_xFe_2O_4$ obtained from the VSM data are 25.0 emu/g, 723.24G, 11.507 emu/gm respectively. As reported [24,25] M_s value for bulk particle of $ZnFe_2O_4$ as 27 emu/g. Therefore the increase in saturation magnetization can be attributed to the effect of nano regime on it. The difference in the value of M_s can be explained in the light of cation distribution. Any change in the concentration and nature of the ions in A and B site should cause resultant magnetization to be different from reported one [26].

3.3. FTIR study

The study of far-infrared spectra is an important tool to get the information about the

position of ions in the crystal [27]. FTIR absorption spectra of the samples in the range of $3.5 \times 10^4 \text{ m}^{-1}$ to $5.8 \times 10^4 \text{ m}^{-1}$ are given in Fig. 9. The spectra show two major absorption bands in the given frequency range. The high and low frequency absorption bands (ν_1 , ν_2) are observed in a frequency range of $5.59 \times 10^4 \text{ m}^{-1}$ to $5.73 \times 10^4 \text{ m}^{-1}$ and $3.54 \times 10^4 \text{ m}^{-1}$ to $4.11 \times 10^4 \text{ m}^{-1}$, which is attributed to tetrahedral and octahedral complexes $Fe^{3+}O^{2-}$. These two bands have been reported by Waldron in spinel structure of ferrite. No shift of absorption band ν_1 is observed. The absorption band ν_2 is slightly shifted to a higher frequency side with addition of R ions and is attributed to increase in bond length on the B-site [28]. This suggests that the rare-earth ions occupy the B-site. The difference in frequencies between ν_1 and ν_2 is due to changes in bond length ($Fe^{3+}O^{2-}$) at tetrahedral and octahedral sites. The broadening of the ν_2 band is observed in rare-earth added $ZnFe_2O_4$, which suggests the occupancy of rare-earth ions on the B-sites.

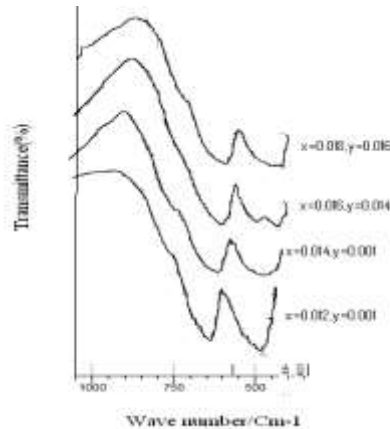


Fig.3 FTIR absorption spectra of the samples.

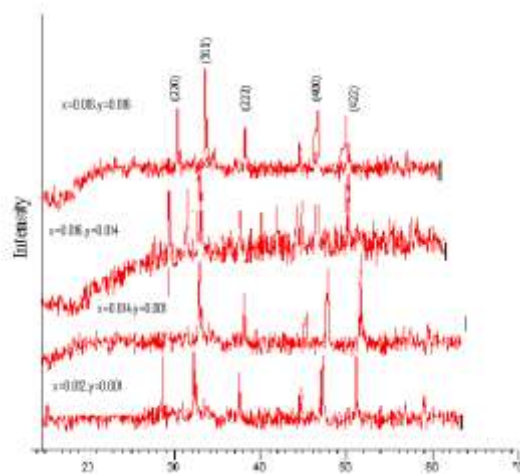


Fig.4 XRD patterns of sintered $Zn_{1-x-y}Co_yCe_xFe_2O_4$, ferrite with different Ce content $x=0.012, 0.014, 0.016, 0.018$ and $y=0.001, 0.001, 0.014, 0.016$

3.4 X-ray diffraction.

Fig.4. shows the X-ray diffraction patterns of pure $ZnFe_2O_4$ and x of cerium ions added to $ZnFe_2O_4$. The X-ray pattern shows reflection plane (220), (311), (222), (400), (422), and (440). It was observed that the appearance of plane (222) is there in all the sample patterns clearly indicate that the pure $ZnFe_2O_4$ shows the presence of single-phase cubic spinel structure. The secondary phase (orthorhombic) is observed in rare-earth ions added Cerium ferrites. The observed secondary phase includes rare earth orthoferrite $CeFeO_3$. It is well known that the degree of replacement of the host cations by the other ions in the host lattice depends on the cations radius of the substituent. The lattice constant a (nm) of spinel structure could be calculated for prominent peak (311) using Bragg's equation

$$a = d_{hkl} \sqrt{h^2 + k^2 + l^2}$$

Where hkl are the indices of mentioned planes.

Lattice constants of all samples prepared in investigation are listed in Table 2. The lattice constant is smaller than pure $ZnFe_2O_4$ and increases with the increase in radius of Ce ions. This is attributed to the large difference between cation radii of R^{3+} and Fe^{3+} owing to the removal of rare-earth ions from the spinel lattice.

The size of crystallite was evaluated by measuring the FWHM of the most intense peak (311) by the Debye Scherrer formula .

$$D = \frac{0.94\lambda}{\beta \cos\theta}$$

XRD patterns exhibit narrow reflection that points to the narrow size crystallites. The results are as shown in Table.2 the mean crystallite

size of the sample lies in the range of 48.38 nm to 76.98 nm. The crystallite size of R ions added sample is smaller than pure Zinc Ferrite.

and coercive force increases with the increase in Ce, these parameters will be very useful for the application of the ferrite materials in the Sensor Studies.

IV. CONCLUSION

From the above experimental results, it is clearly evident that the nano size of the ferrite particles has caused increase in magnetization in Ce doped ZnFe₂O₄. Since Saturation magnetization

Zn _{1-x-y} Co _y Ce _x Fe ₂ O ₄		Ms (emu)	Mag. Mom.	Coercivity (G)	Retentivity (emu)
X=0.012	Y=0.001	0.0769	0.00333	392.95	0.0033
X=0.014	Y=0.001	0.1539	0.00667	147	0.026
X=0.016	Y=0.014	0.214	0.00928	124	0.037
X=0.018	Y=0.016	0.2488	0.0108	155	0.056

Table 1 and 2 shows Ms, Magnetic moment, G, Lattice constant and particle size, Absorption (ν_1 ν_2).

Zn _{1-x-y} Co _y Ce _x Fe ₂ O ₄	Lattice Constant(a Å) A Å	Particle size(D) nm	Absorption/cm ⁻¹ ν_1	Absorption/cm ⁻¹ ν_2
X=0.012, y=0.001	8.32515	76.98	372.25	349.09
X=0.014, y=0.001	8.34459	72.57	381.88	347.16
X=0.016, y=0.014	8.32638	66.96	385.74	362.59
X=0.018, y=0.016	8.342	48.38	383.81	543.89

REFERENCES:

- [1]. N. Iftimie, et.,al, Gas sensitivity of nano crystalline nickel ferrite, *J, Optoelectron and Adv. Mater.* 8(3) (2006) 1016 -1018
- [2]. Ü. Özgür, et.,al, "Microwave Ferrites, Part 1: Fundamental Properties", *J. Mater. Sci.: Materials in Electronics*, (2009) 1-169.
- [3]. Y. Alivov, et.,al, "Microwave Ferrites, Part 2: Passive components and electrical tuning", *J. Mater. Sci.: Materials in Electronics*, (2009)1-169.
- [4]. A.T. Raghavendera, et.,al., Magnetic Properties of Nanocrystalline Al Doped Nickel Ferrite Synthesized by the Sol-Gel Method, *J, Mag and Mag Mat*, 316(1), II (2007) 366-375.
- [5]. H.Gleiter, Synthesis and properties of nanocrystalline nonferrous metals *Prog.Mat.Sci.* 33 (1989) 223-315.
- [6]. J.Smit and H.P.J.Wijn, "Ferrites" *Physical Properties of Ferrimagnetic Oxides in Relation to their technical applications*, Eindhoven: Phillips (1959) p. 142. 4.
- [7]. V.A.M.Barbes, in: *Progress in Spinel Ferrite Research*, H.K.J.Buschow (Ed), Elsevier, Amsterdam, 1995.
- [8]. R.J.Rennard, W.L.Khel, Synthesis, structural characterization and catalytic study. *J.Catal.* 21 (1971) p.282.
- [9]. I.E.Candlish, B.H.Kim, Size-induced effect on nano-crystalline CoFe₂O₄ nanostruct. *Mater.* 1 (1992) p.119.
- [10]. JyotsenduGiri et.,al, Synthesis and magnetic properties of NiFe_{2-x}Al_xO₄ nanoparticles *J.Mater.Chem* 14 (2004) p.875.
- [11]. Sato.H, Umeda.T. et.,al, Synthesis of Magnetic Glass Ceramics Based on Strontium .vol. 34, no. 1, (1993) pp. 76-81.
- [12]. Mathew George, et.,al, *J.Magn.Magn.Mater.* 302 (2006) p.190.
- [13]. Aerdts.R.H.et.,al, 1973.
- [14]. M.Kishimoto, Y.Sakurai, T.Ajima, *J.Appl.Phys.* 76 (1994) 7506.

- [15]. Haitao Xu et.,al, Magnetic properties of Ce,Gd-substituted yttrium iron garnet , J. Mater Proc Tech, Vol.197 (2008) 296-300.
- [16]. F.A.Benko, F.P.Koffyberg, Simple synthesis of MgFe₂O₄ nanoparticles as gas-sensing materials ,Mater.Res.Bull.21, (1986) p.1183.
- [17]. Ru-Qin Yu et.,al, Platinum nanoparticle-modified carbon fiber ultra microelectrodes ,Sensors and Actuators B107,(2005),p.600.
- [18]. Yokoyama.M.,et.,al, Magnetic properties of ultrafine particles and bulk materials of cadmium ferrite, J. Magn. Magn. Mater.,(1998) 183 (1-2): 173.
- [19]. Lee, Y.B., Chae, K., Defect formation in Gd₃Fe₅O₁₂-based garnets: a Mössbauer. J. Phys. Chem. Solids 62, (2001) p.1335.
- [20]. Smith.J et.,al, The effect of highly activated hopping process on the Physical ,Cleaver-Hume Press,(1959).
- [21]. G.M.Bhongale et.,al, EXAFS:Determination of cation distribution in spinels,Bull.Mater.Sci. vol.16, no. 4, (1993) pp. 243-253.
- [22]. Pradeep.A et.,al,Production of single phase nano size NiFe₂O₄ particles using sol-gel auto combustion route by optimizing the preparation conditions,Journal of Magn Mag.Mater, 320 (2008) 2779-278P.
- [23]. Sattar.A et.,al,Rare Earth Doping Effect on the Electrical Properties of cu-Zn Ferrites Journal Physique IV France 7,18-21(1997) 245&246.
- [24]. Kulkarni.R.G,Joshi.H, Comparison of magnetic properties of MgFe₂O₄ prepared by wet-chemical and ceramic methods, Journal.Solid State chem, Volume 64, Issue 2, (1986) 141-147.
- [25]. Khomchenkoa. V.A. et.,al, Effect of Ce substitution on ferroelectric and magnetic properties of BiFeO₃ Scripta Materialia 62, (2010)238- 241.
- [26]. Ashok B.Gadkaria, et.,al, Influence of rare-earth ions on structural and magnetic properties of CdFe₂O₄ ferrites, Chemistry and Materials Science Rare Metals, Vol. 29, No. 2, (2010) 168-173.